

MEMS, Field-Emitter, Thermal, Fluidic Devices & Robotics

Fully 3D-printed, Monolithic, Self-heating Microfluidic Devices	74
Miniaturized Quadrupole Mass Filters via Extrusion for Ionospheric Studies.....	75
Curved Electron Sources for Next-Generation Electron Projection Lithography via Vat Photopolymerization and CNT Drop Casting	76
Silicon Field Emitter Arrays for Vacuum Integrated Circuits.....	77
3D-printed Microfluidic Flow Distributor for Multiplexed Electrospray Droplet Thrusters.....	78
Qualitative Modeling of an Electron Transiting a Vacuum with Drag and Lo-Fi TOE	79
Second Exponential Region in Silicon Nanowire Field Emitter Arrays: Impact Ionization, Direct Band-to-Band Tunneling, or Valence Band Emission?	80
Programmable Current Control of Silicon Field Emitter Arrays Using Gate-all-around MOSFETs.....	81
Field Emitter Arrays Device Characteristics—A Closer Look at Space-charge	82

Fully 3D-printed, Monolithic, Self-heating Microfluidic Devices

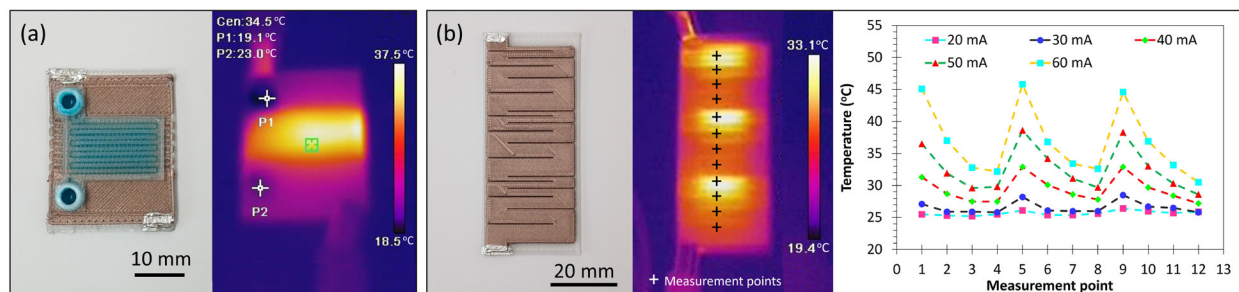
J. Cañada, L. F. Velásquez-García
Sponsorship: Empiriko Corporation, "la Caixa" Foundation

Microfluidic devices allow manipulation and processing of small quantities of fluids by using sub-millimeter scale channels. Microfluidics are used extensively in industry and academia, with applications ranging from drug development to space propulsion. These applications often involve temperature-sensitive processes, e.g., manipulation of living cells, triggering of specific chemical reactions, which make temperature regulation critical. Temperature regulation techniques in microfluidics typically involve the use of bulky equipment external to the microfluidic device, and reports of microfluidics with integrated cooling-heating systems rely on costly fabrication processes and assembly steps.

This work proposes the use of multi-material extrusion three-dimensional (3D) printing to create monolithic, self-heating microfluidic devices in a single, inexpensive manufacturing operation. Material extrusion, also known as fused filament fabrication (FFF), creates parts by heating up feedstock and pushing it through a nozzle, constructing parts layer by layer. Material extrusion, a most accessible additive

manufacturing technology, allows monolithic multi-material fabrication.

The proof-of-concept, self-heating microfluidic devices developed here consist of a 3D-printed resistor that acts as a heat source and a 3D-printed microfluidic channel that directs a fluid from an inlet to an outlet. This simple device demonstrates the ability of multi-material extrusion to produce microfluidic structures with monolithically integrated heating capability. The devices are fabricated using two polylactic acid-based materials: one is dielectric, used to produce the microfluidic channels and structural features; the other is electrically conductive, used to fabricate the resistors that serve as a heat source. The ability of material extrusion to create custom, intricate patterns enables fabrication of complex, application-specific designs of both the microfluidic structure and heating system. Future work includes studying the use of 3D printable materials as temperature sensors to enable closed loop temperature regulation.



▲ Figure 1: (a) Optical and thermal images of a 3D-printed, self-heating microfluidic device, and (b) Optical and thermal images, measured temperature profiles of custom 3D-printed heater.

FURTHER READING

- J. Cañada and L. F. Velásquez-García, "Monolithically 3D-Printed, Self-Heating Microfluidics," *2023 IEEE 22nd International Conference on Micro and Nanotechnology for Power Generation and Energy Conversion Applications (PowerMEMS)*, 2023, pp. 210-213. doi: 10.1109/PowerMEMS59329.2023.10417177.
- A. P. Taylor, J. Izquierdo-Reyes, and L. F. Velásquez-García, "Compact, Magnetically Actuated, Additively Manufactured Pumps for Liquids and Gases," *J. of Physics D—Applied Physics*, vol. 53, no. 35, p. 355002, Aug. 2020. doi: 10.1088/1361-6463/ab8de8
- A. L. Beckwith, L. F. Velásquez-García, and J. T. Borenstein, "Microfluidic Model for Evaluation of Immune Checkpoint Inhibitors in Human Tumors," *Advanced Healthcare Materials*, vol. 8, no. 11, p. 1900289, Jun. 2019. doi: 10.1002/adhm.201900289

Miniaturized Quadrupole Mass Filters via Extrusion for Ionospheric Studies

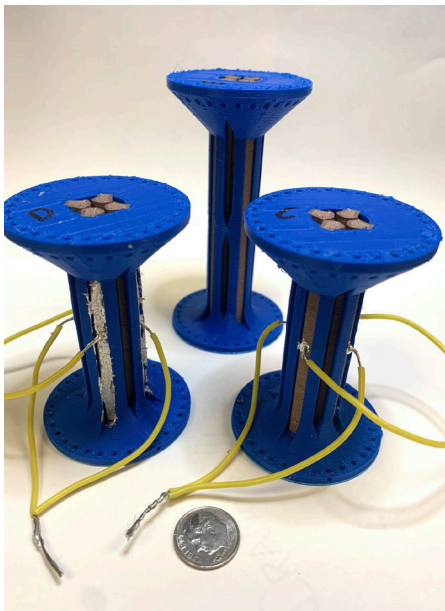
A. Diaz, L. F. Velásquez-García
Sponsorship: MIT Portugal

Mass spectrometry is the gold standard for quantitative chemical analysis. Mass spectrometers employ mass filters that sort out in vacuum the ionized constituents of a sample by mass-to-charge ratio. However, mainstream mass spectrometers are large, heavy, and power-hungry, restricting their ability to be deployed into CubeSats. Mass spectrometer miniaturization has been achieved at the expense of great loss in performance.

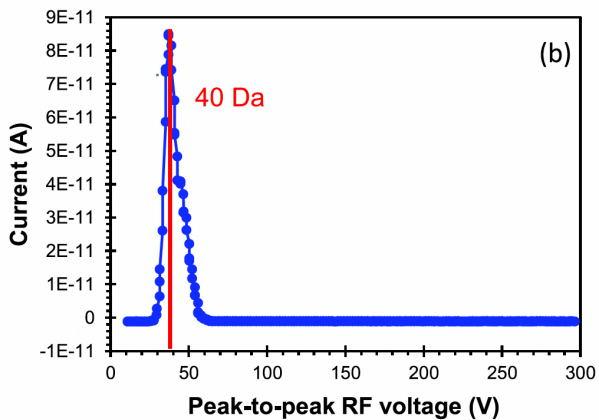
Quadrupoles are a popular choice for a mass filter due to their mass range, resolution, sensitivity, and sturdiness. Quadrupole mass filters use a combination of alternating and direct current voltages to contain species of a given specific charge, transmitting them from one end to the other of the quadrupole. Additive manufacturing makes it possible to create

monolithically and precisely complex objects. Also, additive manufacturing is compatible with in-space manufacturing. Reports of 3D-printed quadrupole mass filters exist, but these are not monolithically made.

In this study, we developed novel, monolithically 3-D-printed quadrupole mass filters with hyperbolic rods (Figure 1). The devices are made via extrusion using polylactic acid (PLA) for the dielectric parts and PLA doped with copper nanoparticles for the conductive structures. The work included the development of compact, low-power, precision electronics to drive devices that are compatible with the size, weight, and power constraints of CubeSats. The devices satisfactorily detect argon—the heaviest gas found in the ionosphere (Figure 2).



▲ Figure 1: Monolithically 3D-printed quadrupole mass filters next to U.S. dime for size comparison.



▲ Figure 2: Mass spectra of argon using a 3D-printed quadrupole mass filter.

FURTHER READING

- A. Diaz and L. F. Velásquez-García, "Compact, Monolithically 3-D Printed Quadrupole Mass Filters for CubeSat Mass Spectrometry," *IEEE Transactions in Instrumentation and Measurement*, vol. 73, pp. 1-10, Mar. 2024. doi: 10.1109/TIM.2024.3372214
- C. C. Eckhoff, N. K. Lubinsky, L. J. Metzler, R. E. Pedder, and L. F. Velásquez-García, "Low-Cost, Compact Quadrupole Mass Filters with Unity Mass Resolution via Ceramic Resin Vat Photopolymerization," *Advanced Science*, vol. 11, no. 9, 2307665, Mar. 2024. doi: 10.1002/adv.202307665
- A. A. Fomani, A. I. Akinwande, and L. F. Velásquez-García, "Resilient, Nanostructured, High-Current, and Low-Voltage Neutralizers for Electric Propulsion of Small Spacecraft in Low Earth Orbit," *IOP J. of Physics: Conference Series*, vol. 476, p. 012014, 2013. doi: 10.1088/1742-6596/476/1/012014

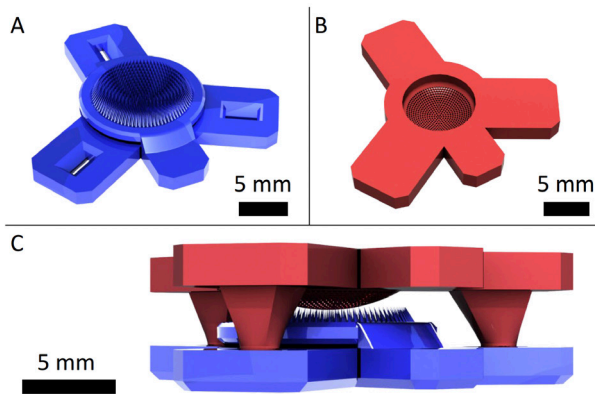
Curved Electron Sources for Next-Generation Electron Projection Lithography via Vat Photopolymerization and CNT Drop Casting

A. Kachkine, L. F. Velásquez-García
Sponsorship: MIT Portugal

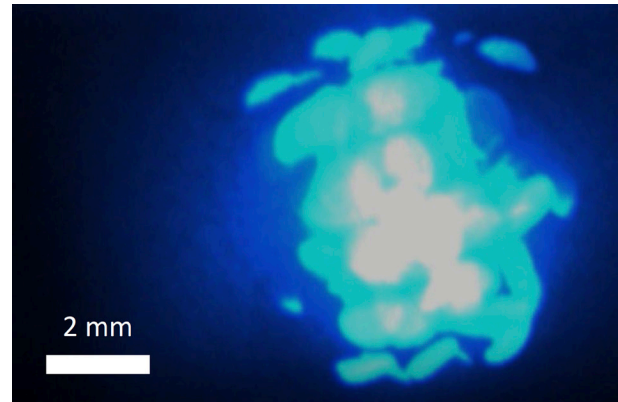
Electron projection lithography (EPL) has the potential to surpass the resolution of mainstream extreme ultraviolet (EUV) lithography for chip manufacturing. Currently, the primary utility of EPL in industry is mask writing for EUV, where EPL beats classic electron beam lithography in terms of throughput. However, development of EPL for chip manufacturing has stalled due to throughput and process uniformity concerns.

We propose a new paradigm for EPL: a confocal electron source (Figure 1). In our design, a monolithic array of micro/nanostructured cones is aligned with an extractor grid; emitted electrons converge onto a collector after a mask, resulting in pattern reduction.

The absence of downstream lenses decreases substrate distance, enabling operation at lower electron energies and potentially increasing resolution. Emission of prototypes made via vat photo-polymerization and carbon nanotube drop casting attain a peak emission current of $300 \mu\text{A}/\text{cm}^2$ (Figure 5). Time-series data shows emission stability. Phosphor screen imaging without a mask shows emission across the entirety of the device (Figure 2). Current research efforts seek to integrate masks into a prototype exposure column, while improving the emission uniformity and optical precision of the electron source.



▲ Figure 1: Renderings of proposed EPL electron source. A) Emitter substrate showing cone decorated, revolved arc surface. B) Extractor with array of apertures. C) Assembled device showing confocal alignment via kinematic couplings.



▲ Figure 2: Phosphor screen image of electron emission.

FURTHER READING

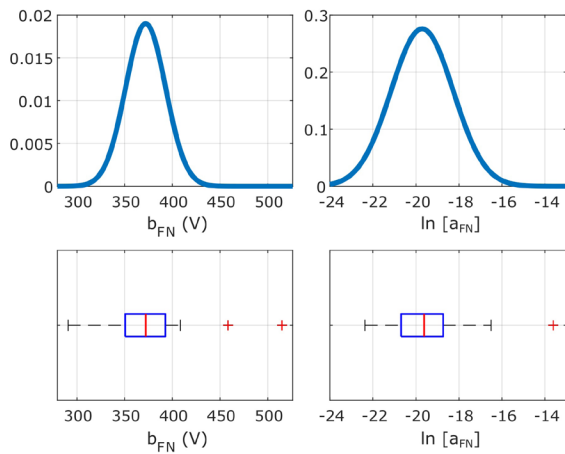
- A. Kachkine, C. E. Owens, A. J. Hart, and Luis F. Velásquez-García, "3D-Printed, Non-Planar Electron Sources for Next-Generation Electron Projection Lithography," *Technical Digest 36th International Vacuum Nanoelectronics Conference (IVNC 2023)*, pp. 128–130, 2023. doi: 10.1109/IVNC57695.2023.10188962
- I. A. Perales-Martinez and L. F. Velásquez-García, "Fully 3D-printed Carbon Nanotube Field Emission Electron Sources with In-plane Gate Electrode," *Nanotechnology*, vol. 30, no. 49, p. 495303, 2019. doi: 10.1088/1361-6528/ab3d17
- C. Yang and L. F. Velásquez-García, "Low-cost, Additively Manufactured Electron Impact Gas Ionizer with CNT Field Emission Cathode for Compact Mass Spectrometry," *Journal of Physics D—Applied Physics*, vol. 52, no. 7, p. 075301, 2019. doi: 10.1088/1361-6463/aaf198

Silicon Field Emitter Arrays for Vacuum Integrated Circuits

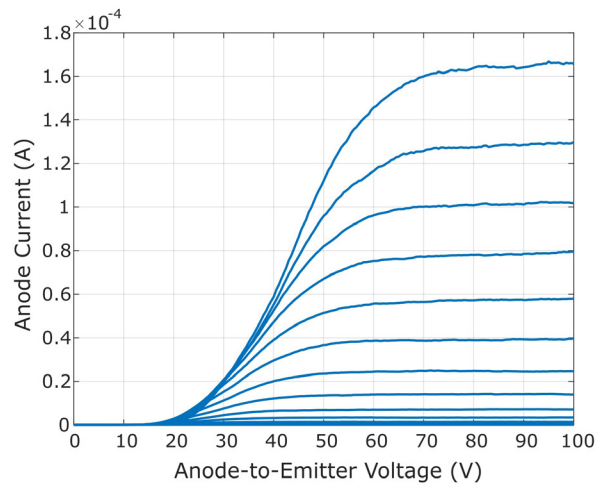
N. Karaulac, A. I. Akinwande
Sponsorship: U.S. Air Force Office of Scientific Research

Nanoscale vacuum-channel transistors are expected to show better performance in a wide variety of high-frequency, high-power, and/or harsh environment applications due to their ballistic transport and higher breakdown field. Silicon field emitter arrays (Si FEAs) are a proven and mature technology that can be implemented as vacuum transistors, and they could also be used in vacuum integrated circuits (ICs). Many of the challenges regarding uniformity, reliability, and lifetime have been addressed in this technology. Most recently, we addressed the scalability of the emission current by designing a layout-independent fabrication process for Si FEAs. However, several questions regarding the feasibility of vacuum ICs remain.

For digital and analog circuits, the transistor parameters must be closely matched, and the impact of variations in a_{FN} and b_{FN} on future vacuum ICs is unknown. In this work, we characterize and model the statistical variation resulting from our fabrication process. In Figure 1, we measure the transfer characteristics of 40 Si FEAs and extract a distribution of a_{FN} and b_{FN} values. We also measure the output characteristics of our devices in Figure 2 and fit the data using a compact model based on a sigmoid (s-shaped) function. Using this model, we perform a Monte Carlo simulation in LTspice of fundamental circuit building blocks, such as an inverter and current mirror, to analyze the impact of the variation of a_{FN} and b_{FN} on future vacuum IC performance.



▲ Figure 1: Box plots showing measured distribution of b_{FN} and $\ln[a_{FN}]$ from 40 Si FEAs ranging in size from single emitter to 1000x1000. Gaussian curves are fitted to the box plots.



▲ Figure 2: Measured output characteristics of 100x100 Si FEA for different values of gate-to-emitter-voltage, V_{GE} . More precisely, $V_{GE} = 20, 22, \dots, 48, 50$ V.

FURTHER READING

- S. A. Guerrero and A. I. Akinwande, "Nanofabrication of Arrays of Silicon Field Emitters with Vertical Silicon Nanowire Current Limiters and Self-aligned Gates," *Nanotechnology*, vol. 27, no. 29, pp. 295302:1-11, Jun. 2016.
- N. Karaulac, G. Rughoobur, and A. I. Akinwande, "Highly Uniform Silicon Field Emitter Arrays Fabricated using a Trilevel Resist Process," *Journal of Vacuum Science & Technology B*, vol. 38, no. 2, pp. 023201:1-7, Jan. 2020.
- N. Karaulac, W. Chern, G. Rughoobur, and A. I. Akinwande, "Silicon Field Emitter Arrays Fabricated using a Layout-independent Process," 2021 34th International Vacuum Nanoelectronics Conference (IVNC), pp. 1-2, 2021.

3D-printed Microfluidic Flow Distributor for Multiplexed Electro spray Droplet Thrusters

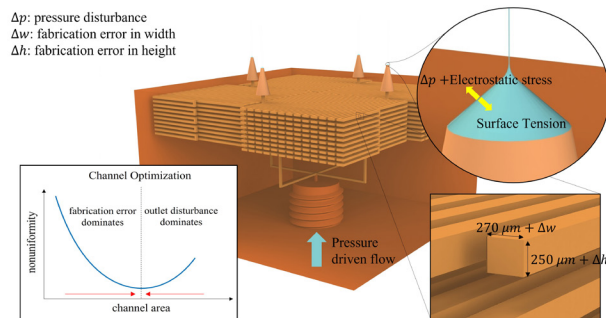
H. Kim, L. F. Velásquez-García
Sponsorship: MIT Portugal

Electrospray propulsion, accomplished by electrohydrodynamically ejecting charged corpuscles of propellant, offers several advantages for propelling small spacecraft like CubeSats. Its capacity to achieve high specific impulse using electrical power rather than being constrained by the chemical energy of the fuel is particularly noteworthy. Also, electrospray thrusters' bipolar emission obviates the need of a neutralizer. However, a single electrospray emitter provides limited thrust because electrospray emission is possible only within a limited range of fuel flow rates. In the higher flow rate regime within this range, the emitted particles are mostly droplets, resulting in higher thrust than the lower flow rate regime emitting ions. Nonetheless, thrust remains constrained, scaling with the flow rate to the power of $\frac{3}{4}$. This thrust constraint necessitates multiple emitters, with uniform operation being crucial to avoid efficiency degradation or emitter flooding. Miniaturization of the electrospray hardware introduces benefits, e.g., lower start-up voltage.

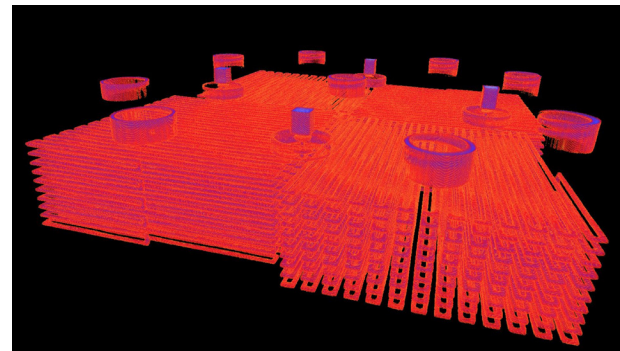
Traditionally, miniaturized electrospray thrusters have been fabricated in a semiconductor cleanroom. However, this method is very expensive,

time-consuming, and incompatible with in-space manufacturing. While 3D-printed, uniformly operating ion-emitting electrospray thruster arrays have been successfully demonstrated, implementing a 3D-printed droplet-emitting thruster has proven challenging. The main challenge lies in fabricating a uniform flow distributor that can tolerate fabrication errors and withstand dynamic outlet conditions caused by non-uniform electric field and interfacial effects, aspects often overlooked by typical bifurcation distributors or other geometries.

To address this challenge, we optimized the design of a uniform flow distributor to cope with fabrication errors and outlet pressure perturbations (Figure 1). Using this framework, we 3D-printed a four-emitter prototype with modified liquid resin capable of printing narrow channels (Figure 2). The prototype exhibited uniform flow distribution while delivering a flow rate up to $\sim 0.1 \text{ mm}^3/\text{s}$ to each emitter of the ionic liquid 1-ethyl-3-methylimidazolium tetrafluoroborate (EMI-BF₄)—a propellant commonly used in electrospray propulsion.



▲ Figure 1: 3D schematic of the flow distributor with sources of non-uniformity explained.



▲ Figure 2: Reconstructed 3D image of the flow distributor from an X-ray microscope.

FURTHER READING

- H. Kim and L. F. Velásquez-García, "Monolithically 3D-Printed Microfluidic Flow Distributor for Uniform Operation of Multiplexed Electro spray Droplet Cubesat Thrusters," *2023 International Conference on Micro and Nanotechnology for Power Generation and Energy Conversion Applications (PowerMEMS)*, pp. 224-227, 2023. doi: 10.1109/PowerMEMS56853.2022.10007598
- A. A. Fomani, A. I. Akinwande, and L. F. Velásquez-García, "Resilient, Nanostructured, High-Current, and Low-Voltage Neutralizers for Electric Propulsion of Small Spacecraft in Low Earth Orbit," *IOP Journal of Physics: Conference Series*, vol. 476, p. 012014, 2013. doi: 10.1088/1742-6596/476/1/012014
- D. Melo Máximo and L. F. Velásquez-García, "Additively Manufactured Electrohydrodynamic Ionic Liquid Pure-Ion Sources for Nanosatellite Propulsion," *Additive Manufacturing*, vol 36, p. 101719, Dec. 2020. doi: 10.1016/j.addma.2020.101719

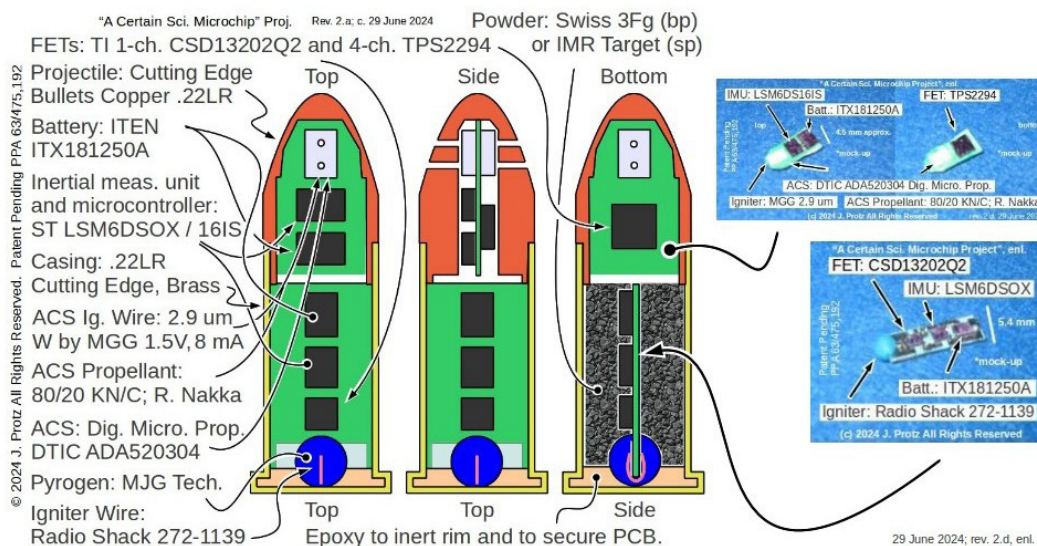
Qualitative Modeling of an Electron Transiting a Vacuum with Drag and Lo-Fi TOE

J. Protz, J. Gerson, P. Kelly, A. Jain, A. Lee

Sponsorship: Protz Lab Group; the former microEngine, LLC and Asteria Propulsion LLC

Study at MIT of the link between the Kalman filter and quantum physics goes back to 1980 and the publication of S. Mitter's LIDS-P-1006; comparable work was published in Japan in 2014 by Ishikawa and Kikuchi and in China in 2022 by Ma, Kong, Wang, and Luand. In 2023, at IVNC at MIT, the present investigator proposed that devices maneuvering in air according to Boyd's energy-maneuverability theory for aircraft (with steady throttle to overcome steady drag, unsteady throttle for maneuver, and throttle lag) could provide an analogy for electrons in the vacuum and that the modeling of groups of such particles might allow the construction of a sort of "lo-fi" fully classical "theory of everything" that reproduces qualitatively many artifacts found in relativity and quantum mechanics and observed experimentally. In the works mentioned above, the irreducible quantum uncertainty of quantum mechanics shows as the driving noise of a system tracked by a Kal-

man filter; here, said driving noise is caused by throttle lag making it not possible to cancel with made thrust the bombardment of the electrons by the smaller particles that compose the vacuum. The project is at an early stage, and the modeling continues; presently, it is focused on making a "video game physics engine". Separately, silicon MEMS propulsion was studied at MIT for two decades; recently, the present investigator has been considering a MEMS chip that would combine a computer, sensors, and a micro rocket motor into a device that could replace a .22 LR bullet's primer cap in NCAA and Olympic competitive sport shooting. A conceptual design has been completed and is illustrated in the figure below. If successful, the project could lead to a class of sport shooting that features teams having both athletes and device engineers in the same way that does auto racing.



▲ Figure 1: conceptual design of a .22 LR digital bullet cartridge for NCAA and Olympic -type sport shooting; chip set used for optical image stabilization (OIS) in digital cameras placed here in casing and used to correct for hand jitter; similar chip set inside projectile enables limited in-flight steering.

FURTHER READING

- J. Protz, "Silicon MEMS DACS and Finite Chord Slender Body Translating in a Vac.," *MIT MTL Annual Research Report 2023*. Abstract. See also poster 3.02 from MIT MTL MARC 2024.
- J. Protz, "Qualitative Modeling of an Electron or Finite-Chord Slender Body Transiting a Vacuum with Drag" P.19 (0087) *36th IEEE IVNC, MIT, 10-13 July 2023* (doi 10.1109/IVNC57695.2023.10188959). Poster.
- J. Protz, Emails to R. Leopold, W. Goldberger, A. Lee, S. M. Spearing, P. Daly, K. Hicks, and others on c. 9 March, 16-17 March, and 9-11 June of 2023 and related files in ~jmplrotz/Public. Personal correspondence.

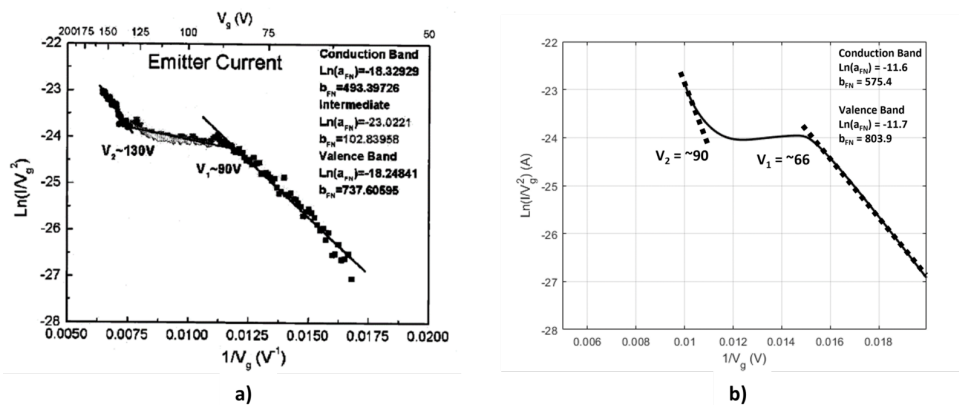
Second Exponential Region in Silicon Nanowire Field Emitter Arrays: Impact Ionization, Direct Band-to-Band Tunneling, or Valence Band Emission?

A. Sahagun, A. I. Akinwande
Sponsorship: U.S. Air Force Office of Scientific Research

At high gate-to-emitter voltages for silicon nanowire field emitter arrays (FEAs), the Fowler-Nordheim (FN) plot shows an unexpected increase in emission current despite the emission current being supply-limited. The second exponential region beyond the supply-limited region in the FN plot might be explained by impact ionization in the semiconductor due to the strong electric field. Other proposals hypothesize that the second exponential region is due to direct band-to-band tunneling resupplying the conduction band for electron emission. However, in the aforementioned cases, the FN slope ($-b_{FN}$) in the second exponential region should remain the same as in the first exponential region; this is not observed experimentally, as shown in Figure 1 a). The difference in the slope of the second exponential region may be due to an increase in the barrier height seen by electrons tunneling from the valence band into vacuum. However, no simulations of this valence band emission have been performed to support this result.

In this work, we aim to simulate the second

exponential region in the field emission current observed experimentally and explore if the second exponential region results from impact ionization, direct band-to-band tunneling, or valence band emission. We use a physics-based approach (SILVACO) to simulate the tunneling probability at both the conduction band and valence band energy levels and the FN slopes. Using SILVACO, we recreated the device structure reported in the literature and simulated it. Preliminary results, shown in Figure 1 b), demonstrate that a sharp increase in emission current exists at high gate-to-emitter voltage after the supply-limited region. Extracting and comparing the slopes of both exponential regions, we find that the ratio is 1.4 in the simulation and 1.49 in the experimental data, which are both close to the suggested slope ratio of 1.45, indicating a two-band field emission model. Additional work explored impact ionization, direct band-to-band tunneling, and valence band emission.



▲ Figure 1: a) Experimental results from a Si NW field emitter with conduction and valence band emission. b) Simulation results from a Si NW field emitter with impact ionization occurring.

FURTHER READING

- M. Ding, H. Kim, and A. I. Akinwande, "Observation of Valence Band Electron Emission from N-type Silicon Field Emitter Arrays," *Applied Physics Letters*, vol. 75, pp. 823–825, Aug. 1999.
- P. G. Borzyak, A. F. Yatsenko, and L. S. Miroshnichenko, "Photo Field Emission from High-resistance Silicon and Germanium," *Physica Status Solidi*, vol. 14, pp. 403–411, Jan. 1966.
- R. N. Thomas and H. C. Nathanson, "Photosensitive Field Emission from Silicon Point Arrays," *Applied Physics Letters*, vol. 21, pp. 384–386, Oct. 1972.

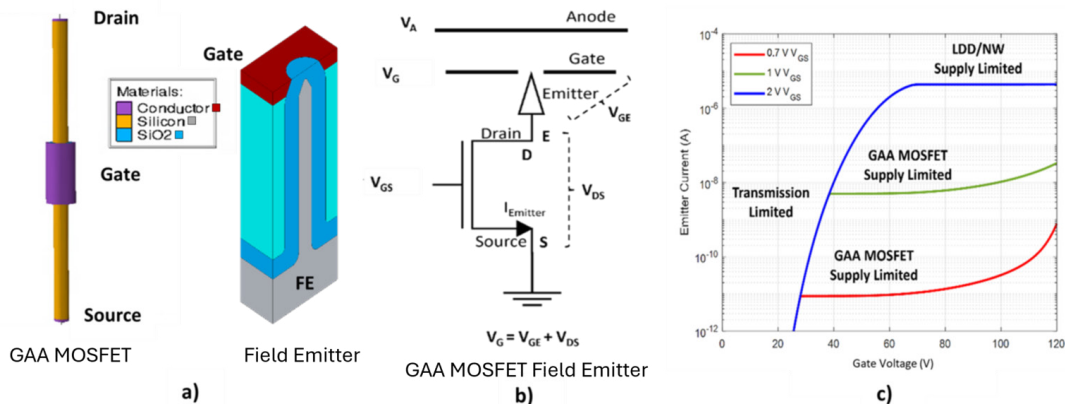
Programmable Current Control of Silicon Field Emitter Arrays Using Gate-all-around MOSFETs

A. Sahagun, A. I. Akinwande

Sponsorship: U.S. Air Force Office of Scientific Research

Silicon field emitter array (FEA) technology has great potential for applications such as electron microscopy, vacuum electronics, and X-ray sources. However, some challenges such as emitter tip burnout and spatial and temporal non-uniformity of emission current impede the adoption of FEAs in these applications. The state-of-the-art approach to addressing these challenges involves integrating a nanowire (NW) current limiter in series with the emitter tips to regulate current flow. The NW current limiter is preferred for its compact integration, which enables high emitter density in FEAs. However, the limiter restricts FEA versatility by constraining the emission current to a fixed maximum value. In contrast, metal-oxide-semiconductor field-effect transistors (MOSFETs) can provide programmable control over emission current. However, integrating planar MOSFETs into FEAs demands significant space, leading to a notable reduction in emitter tip density, FEA compactness, and performance.

In this work, we investigate the integration of vertical gate-all-around (GAA) MOSFETs with individual emitter tips shown in Figure 1 a) and b) to enable programmable emission current control while preserving the compactness, high emitter density, and versatility of FEAs. We use a physics-based approach (SILVACO) to model and simulate the integrated GAA MOSFET-FE device. The simulation results provide insight into the device's I-V characteristics, identifying performance-limiting challenges such as impact ionization occurring in the field emitter and GAA MOSFET. To address the breakdown inherent in GAA MOSFETs, a lightly doped drain, acting essentially as an NW, is included. Preliminary results in Figure 1 c) show the ability of the gate-to-source voltage (V_{GS}) of the GAA MOSFET to transition the field emission process from a transmission-limited region to a supply-limited region.



▲ Figure 1: a) Two individual components: a vertical GAA MOSFET structure obtained in SILVACO and a cutline of a single field emitter from an array with an integrated gate (anode not imaged). b) A series combination of the vertical GAA MOSFET in series with the field emitter. c) Simulation results for GAA MOSFET-FEA I-V characteristics, where V_{GS} is varied from 0.7 V to 2 V.

FURTHER READING

- S. A. Guerrero and A. I. Akinwande, "Nanofabrication of Arrays of Silicon Field Emitters with Vertical Silicon Nanowire Current Limiters and Self-aligned Gates," *Nanotechnology*, vol. 27, pp. 295-302, Jun. 2016.
- C. Y. Hong and A. I. Akinwande, "Temporal and Spatial Current Stability of Smart Field Emission Arrays," *IEEE Transactions on Electron Devices*, vol. 52, pp. 2323-2328, Oct. 2005.

Field Emitter Arrays Device Characteristics—A Closer Look at Space-charge

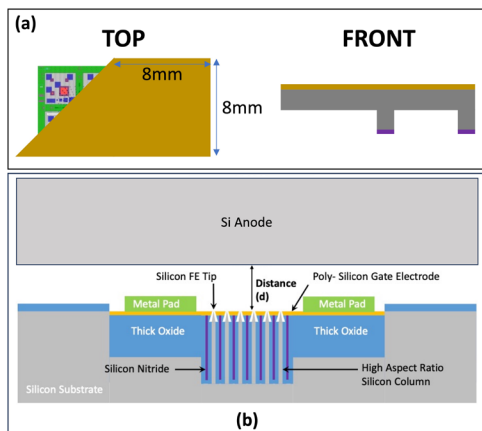
Y. Shin, W. Chern, N. Karaulac, A. I. Akinwande
Sponsorship: AFOSR

Field emitter array- (FEA) based cold cathodes have shown promise as electron sources in devices capable of high power and high frequency operation for a variety of applications such as microwave power amplifiers, pressure sensors, x-ray sources, and high-power excimer lasers. Limited work has explored the device characteristics using well defined cathode-to-anode separation. Consequently, FEAs lack a physics-based compact model.

In this work, a flat stand-off anode was placed on the FEAs, which guarantees the anode distance and the parallel condition. The anode geometry and experimental configuration are shown in Figure 1a. The I-V characteristics in the space charge limit show an unexplained, yet reproducible negative differential resistance (NDR) region (Figure 1b). These results imply that the development of a model for FEAs will need to account for additional phenomena affecting electron

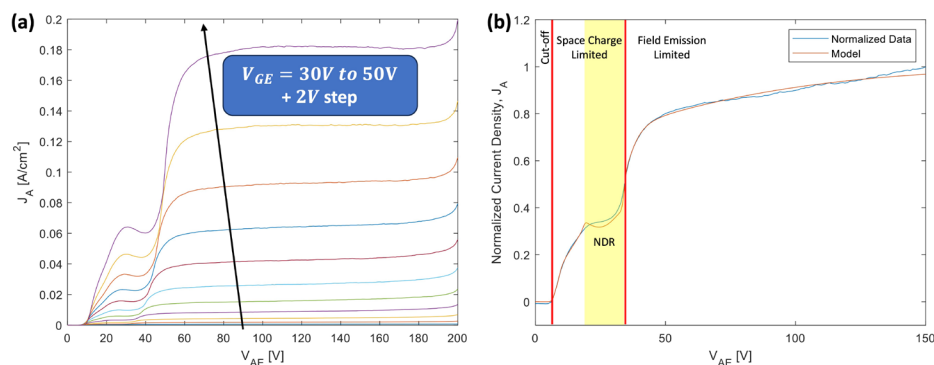
transport in the space between the anode and the gate electrode.

Upon further analysis of the experimental configuration, the electrostatic simulations reveal that a decelerating potential exists in the space between the parallel gate and anode electrodes. The deceleration of the emitted electrons occurs when the anode-to-emitter voltage, V_{AE} , is lower than the gate-to-emitter voltage, V_{GE} . The resulting output characteristics with a fitted model appear in Figure 2. The I-V characteristics were modeled using a semi-empirical approach due to the still ambiguous physical effects caused by the decelerating potential. The model demonstrates good accuracy under typical operating conditions of the experimental configuration. The resulting FEA model opens new avenues of applications including oscillators and amplifiers.



◀ Figure 1: (a) Final anode geometry with proposed integration in relation to device chip and (b) schematic of experimental configuration including details of device structure.

▼ Figure 2: (a) Output characteristic sweep from $V_{GE} = 30V$ to $50V$ and (b) normalized output characteristic of 1000×1000 FEA overlayed by model fitted at $V_{GE} = 34V$. Main operating regimes are labeled; NDR region highlighted.



FURTHER READING

- Y. Shin, "Physics-Based Compact Model Development of Field Emitter Arrays," *Master's thesis, Massachusetts Institute of Technology*, Cambridge, MA, 2024.